

Multiple Eigenvalues Arising from a Class of Repetitive Substructures

Gexue Ren,*Zhaochang Zheng,[†] and Jiangang Cheng[‡]
Tsinghua University, 100084 Beijing, People's Republic of China

The dynamic substructure method in state space was employed to study eigenvalue problems for structures with a class of repetitive substructures, which share a common interface. The block properties of the resulting synthesized system matrices are discussed. A very interesting result on multiple eigenvalues of the considered structures was obtained: each fixed interface eigenvalue of the single repetitive substructure appeared as at least $(n - \alpha)$ multiple eigenvalues of the whole structure, where n is the number of repetitive substructures; α is a number depending on the azimuth distributions of the repetitive substructures. It takes at most nine, and it takes three in the special cases when the repetitive substructures are oriented by rotation around a fixed axis. The mode shapes associated with the $(n - \alpha)$ multiple eigenvalues were obtained and the nondefectiveness of the obtained multiple eigenvalues is discussed. Physical explanation and numerical examples were also attempted and are given.

Nomenclature

C^r	= damping matrix of the r th substructure, symmetric
f^r	= external force vector exerted on the r th substructure
\bar{f}^r	= internal force vector exerted on the interface of the r th substructure
G^r	= gyroscopic matrix of the r th substructure, skew symmetric
i	= indication of internal variables for substructure
j	= indication of interface variables for substructure
K^r	= stiffness matrix of the r th substructure, semipositive definite
M^r	= mass matrix of the r th substructure, positive definite
m_i^r	= internal degree of freedom of the r th substructure
m_j^r	= interface degree of freedom of the r th substructure
m_s^r	= number of retained Jordan blocks for the r th substructure
N	= degree of freedom of the whole structure with the finite element method discretization
s^r	= real or complex numbers used as factors of the fixed interface mode of r th substructure in constructing the modes for the whole structure
T^r	= transformation between the interface coordinates in local coordinate system of the r th substructure and the global interface coordinates system
\bar{T}^r	= transformation matrix between the local coordinate system of the r th substructure and the global displacement system
x^r	= nodal displacement vector for the r th substructure
y_h	= state vector of the common interface in global coordinate system
ζ^r	= third Euler angles used for describing the azimuth of the r th substructure
θ	= first Euler angle used for describing the azimuth of the r th substructure
ξ	= second Euler angle used for describing the azimuth of the r th substructure
ϕ_c^r	= constraint mode matrix of the r th substructure, $2m_i^r \times 2m_j^r$
ϕ_s^r	= right principal mode matrix of the r th substructure with interface being fixed
$\bar{\phi}_s^r$	= left principal mode matrix of the r th substructure with interface being fixed
(Y^r)	= variable related to/of the r th substructure

Introduction

IT is well known that symmetry of structures may lead to multiple eigenvalues; for example, a beam with section and boundary conditions isotropic in two orthogonal directions would result in a series of two multiple eigenvalues. However, in practical test or numerical solutions, close eigenvalues instead of multiple eigenvalues are usually obtained because of the approximate nature of the symmetry being represented by finite precision floating point numbers and manufacturing precision and being solved by test or numerical solution methods. It is not easy to tell whether the closely distributed eigenvalues are close eigenvalues of the original system or multiple eigenvalues themselves. The properties of invariant subspaces associated with multiple eigenvalues make things more unfavorable to the extracting of multiple eigenvalues. In theoretical arithmetic, the second multiplicity of multiple eigenvalues cannot be obtained before a breakdown of the Lanczos process, irrespective of which start vectors are used.¹ However, in finite precision computation, the breakdown rarely happens even for a system with multiple eigenvalues,² and as a compensation, multiple eigenvalues come out multiplicity by multiplicity as close eigenvalues. That is why an inappropriate stop of the Lanczos process would result in missing eigenvalues. Therefore it is of practical importance to use a missing eigenvalue check for missing eigenvalues, especially for structures with multiple eigenvalues. In the case of nonsymmetric eigenvalue problems, such as those encountered in damped structures, the multiple eigenvalues to be solved may be defective. In fact, numerically ascertaining the Jordan structure for defective eigenvalues is very difficult for practical eigenvalue problems.² In general, the study of the arising mechanism of multiple eigenvalues and the development of effective numerical methods for structures with multiple eigenvalues are very important for understanding dynamic characteristics of structures.

The dynamic substructure method or the component mode synthesis method has experienced considerable development, and these concepts have been included in modern texts³⁻⁵ (also see review in Ref. 6). In applying the dynamic substructure method, a structure is first divided into substructures usually according to its geometric characteristics, such as symmetry, repetition, etc.; as a result, the assembled system matrices by the dynamic substructure method have apparent block structures, and the block structures are mappings of topology of substructures in the structure. By taking into account the geometric characteristics of structures, not only can repetitive substructure analyses be omitted but also the geometric topology of the original structure can be retained in the reduced system with the generalized coordinates. The retaining of geometric topology usually retains the eigenstructure of the original system along with the reduced coordinates.

Received May 28, 1996; revision received Sept. 25, 1996; accepted for publication Sept. 27, 1996; also published in *AIAA Journal on Disc*, Volume 2, Number 2. Copyright © 1996 by the American Institute of Aeronautics and Astronautics, Inc. All rights reserved.

*Lecturer, Department of Engineering Mechanics.

[†]Professor, Department of Engineering Mechanics.

[‡]Associate Professor, Department of Engineering Mechanics.

The reason for this research was that in computing the gyroscopic eigenvalue problem of a rotating rotary wing system with four blades, clusters of four close eigenvalues were obtained by numerical methods, and there was no way to tell whether the clustered eigenvalues were multiple eigenvalues or close eigenvalues themselves. Based on the gyroscopic mode synthesis technique developed by Zheng and Wu,⁷ it was found that there should be $(n - 3)$ multiple eigenvalues in each cluster, where n is the number of blades in the rotary wing model.⁸ Further studies show that a class of more general repetitive substructures possesses multiple eigenvalues due to the repetition of its substructures.

Dynamic Substructure Method for Structures with a Class of Repetitive Substructures

Structures with repetitive substructures are ubiquitous in engineering. One class of such structures has repetitive substructures that share a common interface and all of the repetitive substructures are mounted on the rest of the structure through the interface, such as the rotary wing model shown in Fig. 1, the antenna structure shown in Fig. 2, and the man-made fountain models, which are very common in modern cities, as shown in Fig. 3. For analyses of structures with repetitive substructures, it is often expedient to use dynamic substructure methods. Denoting the n repetitive substructures, respectively, as the first, second, \dots , and the n th substructure and the rest of the structure as the $(n + 1)$ th substructure, generally, the equation of motion for the r th substructure can be written as

$$M^r \ddot{x}^r + (G^r + C^r) \dot{x}^r + K^r x^r = f^r + \bar{f}^r \quad (r = 1, \dots, n + 1) \quad (1a)$$

The resulting equations of motion of damped rotating structures such as the rotary wing system may take the form of Eq. (1a), due to the presence of Coriolis forces in the rotating coordinate system. Equation (1a) can also be used for nonrotating, undamped structures with the vanishing of the gyroscopic matrix G^r and/or the damping matrix C^r .

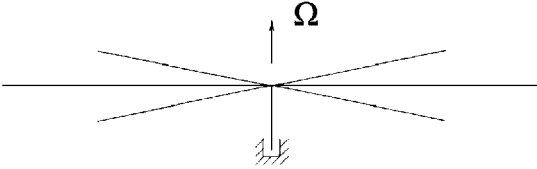


Fig. 1 Rotary wing model.

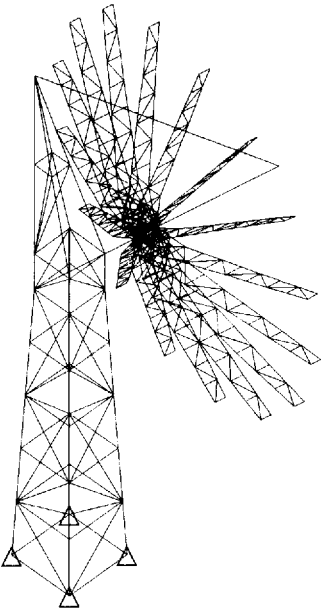


Fig. 2 Antenna model.

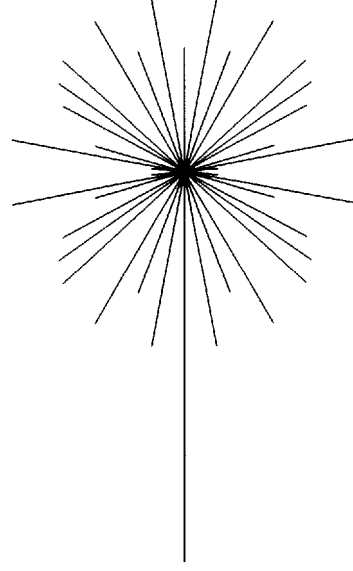


Fig. 3 Man-made fountain model.

For applying the dynamic substructure method, Eq. (1a) was partitioned according to the internal and interface coordinates, i.e.,

$$\begin{bmatrix} M_{ii}^r & M_{ij}^r \\ M_{ji}^r & M_{jj}^r \end{bmatrix} \begin{Bmatrix} \ddot{x}_i^r \\ \ddot{x}_j^r \end{Bmatrix} + \left(\begin{bmatrix} G_{ii}^r & G_{ij}^r \\ G_{ji}^r & G_{jj}^r \end{bmatrix} + \begin{bmatrix} C_{ii}^r & C_{ij}^r \\ C_{ji}^r & C_{jj}^r \end{bmatrix} \right) \begin{Bmatrix} \dot{x}_i^r \\ \dot{x}_j^r \end{Bmatrix} + \begin{bmatrix} K_{ii}^r & K_{ij}^r \\ K_{ji}^r & K_{jj}^r \end{bmatrix} \begin{Bmatrix} x_i^r \\ x_j^r \end{Bmatrix} = \begin{Bmatrix} f_i^r \\ f_j^r \end{Bmatrix} + \begin{Bmatrix} 0 \\ \bar{f}_j^r \end{Bmatrix} \quad (1b)$$

To avoid treating the resulting quadratic eigenvalue problem for Eq. (1b), Eq. (1b) can be transformed into its state-space form⁷:

$$\begin{bmatrix} A_{ii}^r & A_{ij}^r \\ A_{ji}^r & A_{jj}^r \end{bmatrix} \begin{Bmatrix} \dot{y}_i^r \\ \dot{y}_j^r \end{Bmatrix} + \begin{bmatrix} B_{ii}^r & B_{ij}^r \\ B_{ji}^r & B_{jj}^r \end{bmatrix} \begin{Bmatrix} y_i^r \\ y_j^r \end{Bmatrix} = \begin{Bmatrix} F_i^r \\ F_j^r \end{Bmatrix} + \begin{Bmatrix} 0 \\ \bar{F}_j^r \end{Bmatrix} \quad (2)$$

where

$$A_{kl}^r = \begin{bmatrix} (G_{kl}^r + C_{kl}^r) & M_{kl}^r \\ -M_{kl}^r & 0 \end{bmatrix}, \quad B_{kl}^r = \begin{bmatrix} K_{kl}^r & \\ & M_{kl}^r \end{bmatrix}$$

$$y_k^r = \begin{Bmatrix} x_k^r \\ \dot{x}_k^r \end{Bmatrix}, \quad F_k^r = \begin{Bmatrix} f_k^r \\ 0 \end{Bmatrix}$$

$$\bar{F}_k^r = \begin{Bmatrix} \bar{f}_k^r \\ 0 \end{Bmatrix} \quad (k, l = i, j)$$

As a generalization of the fixed interface method in state space, the following transformations between state variables and the generalized coordinates \bar{y}^r for the r th substructure are introduced:

$$\begin{Bmatrix} y_i^r \\ y_j^r \end{Bmatrix} = \begin{bmatrix} \phi_i^r & \phi_j^r \\ 0 & I \end{bmatrix} \begin{Bmatrix} q^r \\ y_j^r \end{Bmatrix} = \Psi^r \bar{y}^r \quad (r = 1, \dots, n + 1) \quad (3)$$

where

$$\phi_c^r = \begin{bmatrix} (K_{ii}^r)^{-1} K_{ij}^r & \\ & (K_{ii}^r)^{-1} K_{ij}^r \end{bmatrix}$$

and where ϕ_i^r and $\bar{\phi}_i^r$ can be obtained by the following substructure analysis. With the interface being fixed, B_{ii}^r is usually positive definite. Doing the Cholesky decomposition of B_{ii}^r ,

$$B_{ii}^r = L_B^r (L_B^r)^T \quad (4)$$

The eigensolution of $(L_B^r)^{-1} A_{ii}^r (L_B^r)^{-T}$

$$(X_{ii}^r)^{-1} [(L_B^r)^{-1} A_{ii}^r (L_B^r)^{-T}] X_{ii}^r = \text{block_diag} \{J_1^r, J_2^r, \dots, J_{m_s^r}^r\} = \Lambda^r \quad (5)$$

where Λ^r is a principal submatrix of the Jordan form of $(L_B^r)^{-1} A_{ii}^r (L_B^r)^{-T}$, with the Jordan blocks

$$J_k^r = \begin{bmatrix} \lambda_k^r & 1 & & \\ & \lambda_k^r & \ddots & \\ & & \ddots & 1 \\ & & & \lambda_k^r \end{bmatrix} \quad (k = 1, \dots, m_s^r) \quad (6)$$

being ordered from lower to higher frequencies.

Defining $\phi_s^r = (L_B^r)^{-T} X_{ii}^r$ and $\bar{\phi}_s^r = (X_{ii}^r)^{-1} (L_B^r)^{-1}$, we have

$$(\bar{\phi}_s^r)^T A_{ii}^r \phi_s^r = \Lambda^r \quad (7a)$$

$$(\bar{\phi}_s^r)^T B_{ii}^r \phi_s^r = I^r \quad (7b)$$

and

$$A_{ii}^r \phi_s^r = B \phi_s^r \Lambda^r \quad (8)$$

Substituting Eq. (3) into Eq. (2) and premultiplying it with $(\bar{\Psi}^r)^T$, we have

$$\bar{T}^r = \begin{bmatrix} \cos \xi^r \cos \zeta^r - \sin \xi^r \cos \theta^r \sin \zeta^r & \sin \xi^r \cos \zeta^r + \cos \xi^r \cos \theta^r \sin \zeta^r & \sin \theta^r \sin \zeta^r \\ -\cos \xi^r \sin \zeta^r - \sin \xi^r \cos \theta^r \cos \zeta^r & -\sin \xi^r \sin \zeta^r + \cos \xi^r \cos \theta^r \cos \zeta^r & \sin \theta^r \cos \zeta^r \\ \sin \xi^r \sin \theta^r & -\cos \xi^r \sin \theta^r & \cos \theta^r \end{bmatrix} \quad (11)$$

$$\bar{A}^r \bar{y}^r + \bar{B}^r \bar{y}^r = \bar{F}^r + \bar{F}_j^r \quad (r = 1, \dots, n+1) \quad (9)$$

where

$$\bar{A}^r = (\bar{\Psi}^r)^T A^r \Psi^r = \begin{bmatrix} \Lambda^r & \bar{A}_{ij}^r \\ \bar{A}_{ji}^r & \bar{A}_{jj}^r \end{bmatrix}$$

$$\bar{B}^r = (\bar{\Psi}^r)^T B^r \Psi^r = \begin{bmatrix} I^r & B_{ij}^r \\ B_{ji}^r & B_{jj}^r \end{bmatrix}, \quad \bar{F}^r = (\bar{\Psi}^r)^T \begin{Bmatrix} F_i^r \\ F_j^r \end{Bmatrix}$$

$$\hat{F}_j^r = (\bar{\Psi}^r)^T \begin{Bmatrix} 0 \\ \bar{F}_j^r \end{Bmatrix}, \quad \bar{\Psi}^r = \begin{bmatrix} \bar{\phi}_s^r & \phi_k^r \\ 0 & I \end{bmatrix}$$

Other dynamic substructure methods in physical space can also be generalized into state-space form. The adoption of the fixed interface method proves itself appropriate for the class of repetitive substructures that possess a common interface, as will be shown in the following sections.

The synthesized global equation for the structure can be obtained by enforcing the compatibility and equilibrium conditions on the common interface of the substructures, i.e.,

$$T^1 y_j^1 = T^2 y_j^2 = \dots = T^n y_j^n = T^{n+1} y_j^{n+1} = y_h \quad (9a)$$

$$\sum_{r=1}^{n+1} T^r \hat{F}_j^r = 0 \quad (9b)$$

The resulting synthesized global equation is

$$\tilde{A} \tilde{y} + \tilde{B} \tilde{y} = \tilde{F} \quad (10)$$

where

$$\tilde{A} = \begin{bmatrix} \Lambda^1 & & & \bar{A}_{ij}^1 (T^1)^T \\ & \ddots & & \vdots \\ & & \Lambda^n & \bar{A}_{ij}^n (T^n)^T \\ & & & \Lambda^{n+1} \bar{A}_{ij}^{n+1} (T^{n+1})^T \\ T^1 \bar{A}_{ji}^1 & \dots & T^n \bar{A}_{ji}^n & T^{n+1} \bar{A}_{ji}^{n+1} \sum_{r=1}^{n+1} T^r \bar{A}_{jj}^r (T^r)^T \end{bmatrix}$$

$$\tilde{B} = \begin{bmatrix} I^1 & & & \bar{B}_{ij}^1 (T^1)^T \\ & \ddots & & \vdots \\ & & I^n & \bar{B}_{ij}^n (T^n)^T \\ & & & I^{n+1} \bar{B}_{ij}^{n+1} (T^{n+1})^T \\ T^1 \bar{B}_{ji}^1 & \dots & T^n \bar{B}_{ji}^n & T^{n+1} \bar{B}_{ji}^{n+1} \sum_{r=1}^{n+1} T^r \bar{B}_{jj}^r (T^r)^T \end{bmatrix}$$

$$\tilde{y} = \begin{Bmatrix} q^1 \\ \vdots \\ q^{n+1} \\ y_h \end{Bmatrix}, \quad T^r = \begin{bmatrix} \bar{T}^r & & \\ & \bar{T}^r & \\ & & \ddots \\ & & & \bar{T}^r \end{bmatrix} \quad (r = 1, \dots, n)$$

As a coordinate transformation matrix, \bar{T}^r can be expressed in terms of Euler angles without loss of generality, i.e.,

Obviously, the synthesized system matrices \tilde{A} and \tilde{B} possess block properties, which are determined by the way in which the structure is partitioned into substructures and the dynamic substructure being used. Usually, symmetry and repetition of the original structure are taken into consideration in the partitioning. Hence the geometric characteristics of the original structure are generally embedded in the block structure of the synthesized system matrices. The block structure of the synthesized system matrices carries an important character; i.e., it remains invariant irrespective of how many fixed interface modes are retained for the substructures. This character demonstrates that the geometric properties of the original system are retained along with the generalized coordinates in the synthesized system, though the degrees of freedom (DOFs) of the system may be reduced. With the block properties of the synthesized system matrices by dynamic substructure method, it is possible to discuss the qualitative properties of the dynamic characteristics of the system. The conclusion in the next section was obtained by following this idea.

Result on Multiple Eigenvalues Arising from the Repetitive Substructures

Theorem 1: For a structure having n repetitive substructures with a common interface, with the repetitive substructures mounted on the rest of the structure through the common interface, then 1) corresponding to every fixed interface mode of the repetitive substructure, the whole structure has $(n - \alpha)$ independent mode shapes, which are combinations of the mode of the repetitive substructure, where α is a number depending on the azimuth distribution of the repetitive substructures. It takes three for the case of the repetitive substructures oriented by rotations around a fixed axis, and it takes at most nine for arbitrary azimuth distributions of the repetitive substructures. 2) Each eigenvalue of the repetitive substructure with the interface fixed is at least $(n - \alpha)$ multiple eigenvalues of the whole structure, and α is determined as in 1).

provided that the corresponding eigenvalues of the repetitive substructure were not defective. The Jordan blocks of the repetitive substructure are only repeated as simple eigenvalues being repeated without introducing new defectiveness to the eigenvalue problem of the whole structure.

Numerical Examples

Example 1: Rotating Rotary Wing Models

The systems were studied in the noninertial coordinate systems that are fixed on the rotating rotary wing models, and so the resulting eigenvalue problems are gyroscopic eigenvalue problems due to the presence of the Coriolis forces. The computed frequencies for the single blade and the four, six, and nine isotropically distributed bladed rotary wing models are described in Tables 1, 2, 3, and 4, respectively. From the boldfaced frequencies in the tables, each frequency of the single blade is, respectively, one, three, and six multiple eigenvalues of the four-, six-, and nine-bladed rotary wing model, which completely agrees with the obtained analytical results. The computed results for two rotating rotary wing models with six nonisotropically distributed blades (Figs. 4a and 4b) are shown in Tables 5 and 6. In the latter model, there was also a pitched angle

Table 1 First four frequencies of the blade with its root being fixed

Frequency, rad/s			
80.3691	494.746	1230.09	1998.03

Table 2 First 16 frequencies of the four-bladed rotary wing model

Frequency, rad/s			
80.3485	80.3485	80.3672	80.3691
494.684	494.684	494.735	494.746
1229.91	1229.91	1230.04	1230.09
1477.94	1957.26	1973.66	1998.04

Table 3 First 24 frequencies of the six-bladed rotary wing model

Frequency, rad/s			
80.3382	80.3383	80.3663	80.3691
80.3691	80.3691	494.653	494.653
494.730	494.746	494.746	494.746
1229.81	1229.82	1230.01	1230.09
1230.09	1230.09	1333.40	1935.46
1960.67	1998.04	1998.04	1998.04

Table 4 First 36 frequencies of the nine-bladed rotary wing model

Frequency, rad/s			
80.3228	80.3228	80.3649	80.3691
80.3691	80.3691	80.3691	80.3691
80.3691	494.605	494.607	494.723
494.746	494.746	494.746	494.746
494.746	494.746	1178.66	1229.66
1229.68	1229.97	1230.09	1230.09
1230.09	1230.09	1230.09	1230.09
1901.15	1940.21	1998.04	1998.04
1998.04	1998.04	1998.04	1998.04

Table 5 First 24 frequencies of the six-bladed (nonisotropic) model

Frequency, rad/s			
80.0162	80.0992	80.3458	80.3691
80.3691	80.3691	493.579	493.869
494.620	494.746	494.746	494.746
539.375	1219.47	1225.43	1229.41
1230.09	1230.09	1230.09	1337.40
1546.17	1998.04	1998.04	1998.04

Table 6 First 24 frequencies of the six-bladed (nonisotropic, $\beta = 30$ deg) model

Frequency, rad/s			
79.9172	80.1290	80.3162	80.3691
80.3691	80.3691	492.901	493.973
494.514	494.746	494.746	494.746
561.884	1216.33	1226.00	1229.26
1230.09	1230.09	1230.09	1425.84
1634.78	1998.04	1998.04	1998.04

Table 7 Frequencies of the single repetitive substructure with fixed interface

Frequency, rad/s				
0.313532	1.82593	4.18062	4.96736	9.04258

Table 8 First 40 eigenfrequencies of the whole structure

Frequency, rad/s				
0.049878	0.068221	0.105353	0.313532	0.313532
0.313532	0.313532	0.313532	0.313532	0.313532
0.313532	0.313532	0.313532	0.313532	0.313532
0.313532	0.321168	0.324065	0.404079	0.717778
0.725019	1.22493	1.82593	1.82593	1.82593
1.82593	1.82593	1.82593	1.82593	1.82593
1.82593	1.82593	1.82593	1.82593	1.82593
1.98248	1.99341	1.99577	3.72978	4.18062

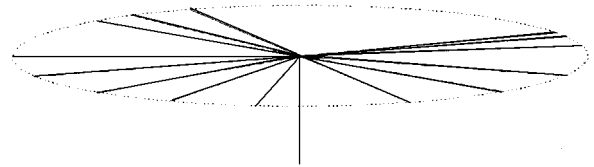


Fig. 4a Model with nonisotropically distributed blades.

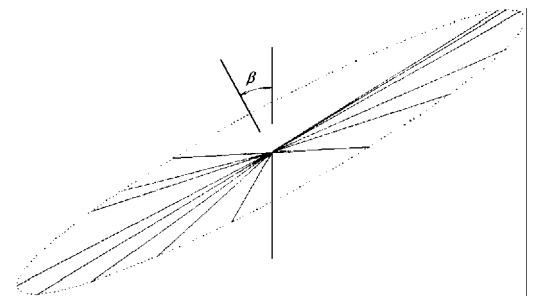


Fig. 4b Model with pitched nonisotropically distributed blades.

$\beta = 30$ deg, and the rotating of the rotary wing was around the direction that is pitched from the original shaft axis. From the boldfaced frequencies in Tables 5 and 6, each frequency of the single blade appears as three multiple eigenvalues of rotary wing models with six nonisotropically distributed blades, which completely agrees with the analytical results. The azimuthal angles of the blades were 0, 45, 105, 120, 240, and 320 deg.

Blade material and section parameters were $E = 2.1 \times 10^{11}$ Pa, $\nu = 0.3$, $J_y = 1.167 \times 10^{-11}$ m⁴, $J_z = 1.167 \times 10^{-8}$ m⁴, $\rho = 1.13 \times 10^{-1}$ kg/m, and $A = 2.231 \times 10^{-5}$ m². Shaft material and section parameters were $E = 2.1 \times 10^{12}$ Pa, $\nu = 0.3$, $J_y = J_z = 1.167 \times 10^{-8}$ m⁴, $\rho = 1.13 \times 10^{-1}$ kg/m, and $A = 2.231 \times 10^{-5}$ m². The length of the blade and the shaft were, respectively, 0.508 and 0.2 m. Five uniform beam elements were used for the discretization of the blade, and two elements were used for the shaft. Rotating speed was $\Omega = 1200$ rpm.

There were also examples on damped gyroscopic eigenvalue problems by Zheng and Ren¹⁰ and Ren,¹¹ the results of which agree with the analytical results in this paper.

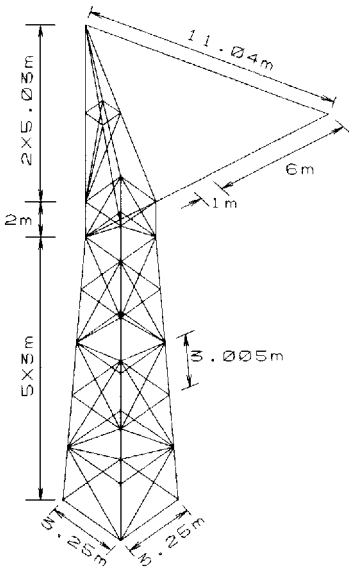


Fig. 5a Repetitive substructure of the antenna model.

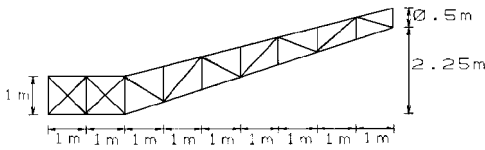


Fig. 5b Nonrepetitive substructure of the antenna model.

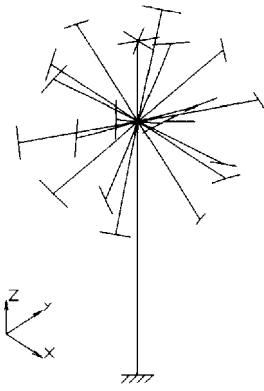


Fig. 6 Fountain model.

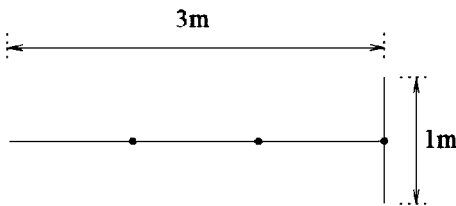


Fig. 7 Repetitive substructure of the fountain model.

Example 2: An Antenna Model

Figure 2 shows an antenna model, the dimensions of which are shown in Figs. 5a and 5b. All of the beam members in the structure have the same material and section properties: $E = 2.1 \times 10^{11}$ Pa, $\nu = 0.3$, $\rho = 7800$ kg/m³, $A = 0.09$ m², and $J_y = J_z = 2.5 \times 10^{-9}$ m⁴. The numerical results by subspace iteration for the eigenfrequencies of the single repetitive substructure and the whole structure are shown in Tables 7 and 8. There were 16 repetitive substructures in the model that are distributed around an axis. This model satisfies the conditions for the $(n - 3)$ multiple eigenvalues in Theorem 1. From the boldfaced frequencies in Table 8, the frequencies of the single repetitive structure do appear as 13 multiple eigenvalues of the whole structure.

Table 9 First 23 frequencies of the fountain model

Frequency, rad/s			
0.00576174	0.00576184	0.0174299	0.0381241
0.0381241	0.164308	0.164308	0.225159
0.225159	0.225159	0.225159	0.225159
0.225159	0.225159	0.225160	0.225160
0.225160	0.225160	0.225160	0.225160
0.225495	0.225763	0.226071	0.226364
0.226646	2.27001	2.27001	2.27001
2.27001	2.27001	2.27001	2.27001
2.27001	2.27001	2.27001	2.27001
2.27001	2.27001	2.32065	2.32067

Table 10 Frequencies of the repetitive substructure with fixed interface

Frequency, rad/s	
0.225159	0.227001

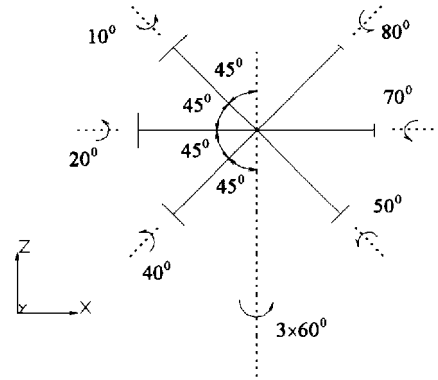


Fig. 8a Generation of repetitive substructures in the fountain model.

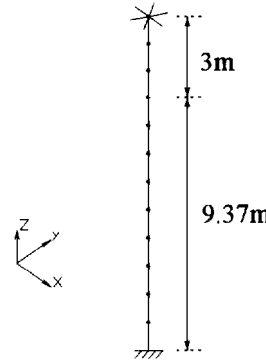


Fig. 8b Nonrepetitive substructure of the fountain model.

Example 3: Fountain Model

Figure 6 shows a fountain model. The repetitive substructure, its 18 repetitions in the structure, and the finite element method discretization are shown in Figs. 7, 8a, and 8b, respectively. The computed eigen-frequencies for the fountain model and the repetitive substructure (fixed interface) are described in Tables 9 and 10, respectively. From the boldfaced frequencies in Table 9, each frequency of the single repetitive substructure appeared, numerically, as 13 multiple eigenvalues of the whole structure. The multiplicity of the eigenvalues was obviously larger than the least value $9 = (18 - 9)$ that is given in Theorem 1. The computed results show that $\alpha = 9$ is too conservative for the considered structure. This is mainly because the DOFs of the common interface of the repetitive substructures are not confined in the proof of the theorem; however, the DOF of the interface in the present example model is only that for one beam node, i.e., six. If this condition is taken into consideration, the least multiplicity for this example could be refined to $(n - 6)$ by reconsidering the proof for Theorem 1. Each beam member in the computational model has the same material and section parameters: $E = 7 \times 10^{10}$ Pa, $\nu = 0.3$, $\rho = 2700$ kg/m³, $A = 0.001$ m², and $J_y = J_z = 2.5 \times 10^{-11}$ m⁴.

Conclusion

In terms of the block structure of the synthesized system matrices by the dynamic substructure method, the fact that multiple eigenvalues stem from the class of repetitive substructures that share a common interface has been found out analytically. The multiplicity of the multiple eigenvalues turns out to depend on the azimuthal distributions of the repetitive substructures. Furthermore, such multiple eigenvalues arising from symmetry or repetition in geometry of the structure do not introduce new defectiveness to the eigenvalue problem of the system, irrespective of whether the considered system is undamped or damped, nongyroscopic or gyroscopic. The symmetry or structure retaining property of the dynamic substructure method is an advantage over other raw reduction eigenvalue methods, and it deserves further attention.

Acknowledgments

This research was supported by the National Natural Science Foundation of the People's Republic of China and the Doctoral Training Foundation of Education Committee of the People's Republic of China.

References

¹Wilkinson, J. H., *The Algebraic Eigenvalue Problem*, Clarendon, Oxford, England, UK, 1965, pp. 369–377.

²Golub, G. H., and Van Loan, C. F., *Matrix Computations*, Johns Hopkins Univ. Press, Baltimore, MD, 1989, pp. 390–392, 484–489.

³Craig, R. R., *Structural Dynamics*, Wiley, New York, 1981, Chap. 19.

⁴Meirovitch, L., *Computational Methods in Structural Dynamics*, Sijthoff and Noordhoff, Alphen aan den Rijn, The Netherlands, 1980, Chap. 11.

⁵Ewins, D. J., *Modal Testing: Theory and Practice*, Research Studies Press, Letchworth, England, UK, 1984, Chap. 6.

⁶Greif, R., “Substructuring and Component Mode Synthesis,” *Shock and Vibration Digest*, Vol. 18, No. 7, 1986, pp. 3–8.

⁷Zheng, Z. C., Zhou, X. P., and Li, D. B., “Gyroscopic Mode Synthesis in the Dynamic Analysis of a Multi-Shaft Rotor-Bearing Systems,” American Society of Mechanical Engineers, ASME 85-IGT-73, Beijing, PRC, Sept. 1985, pp. 1–7.

⁸Ren, G., *Numerical Methods for Large Scale Gyroscopic Eigenvalue Problems*, Tsinghua Univ., Beijing, PRC, 1993, pp. 75–90.

⁹Newland, D. E., *Mechanical Vibration Analysis and Computation*, Longman Scientific and Technical, Singapore, 1989, pp. 185–191.

¹⁰Zheng, Z. C., and Ren, G. X., “Large Scale Non-Symmetric Eigenvalue Problem in Structural Dynamics,” *Proceedings of the 13th International Modal Analysis Conference*, Society for Experimental Mechanics, Bethel, CT, 1995, pp. 1622–1629.

¹¹Ren, G. X., “Method for Large Scale Non-Classically Damped Eigenvalue Problem, Part-I, A Material Reduction Algorithm, Part-II, A Restart Technique,” Postdoctoral Research Rept., Tsinghua Univ., Beijing, PRC, 1995, pp. 20–55; see also *International Journal for Numerical Methods in Engineering* (submitted for publication).